Journal of Power Sources 198 (2012) 100–104

Contents lists available at SciVerse ScienceDirect

Journal of Power Sources

journal homepage: www.elsevier.com/locate/jpowsour

Short communication

The effect of water proofing on the performance of nickel foam cathode in microbial fuel cells

Jia Liu[a], Yujie Feng[a,*], Xin Wang[b], Qiao Yang[a], Xinxin Shi[a], Youpeng Qu[a], Nanqi Ren[a]

[a] State Key Laboratory of Urban Water Resource and Environment, Harbin Institute of Technology, No 73 Huanghe Road, Nangang District, Harbin 150090, China
[b] MOE Key Laboratory of Pollution Processes and Environmental Criteria, College of Environmental Science and Engineering, Nankai University, Tianjin 300071, China

ARTICLE INFO

Article history:
Received 11 August 2011
Received in revised form
23 September 2011
Accepted 24 September 2011
Available online 1 October 2011

Keywords:
Microbial fuel cells (MFCs)
Nickel foam
Wet proofed
Corrosion inhibition
Power density

ABSTRACT

The long-term stability of inexpensive metal matrix of cathodes is one of the most important factors limiting the scaling-up of air-cathode microbial fuel cells (MFCs). We demonstrate that the wet proofing by polytetrafluoroethylene (PTFE) increases the performance of nickel foam cathode in MFCs. After the water proofing is applying on the nickel foam (Ni-W), a corrosion inhibition efficiency of 97% is obtained by the measurements of potentiodynamic polarization. Using Pt as the catalyst, the maximum power density of MFC using wet proofed cathode (Ni-W-Pt) is $0.69 \pm 0.01\,W\,m^{-2}$, with a value of 35% higher than $0.51 \pm 0.01\,W\,m^{-2}$ of non-wet proofed cathode (Ni-NW-Pt). Oxygen mass transfer coefficient (k) of Ni-W-Pt cathodes is $0.68 \pm 0.06 \times 10^{-4}\,cm\,s^{-1}$, which is 53% lower than $1.46 \pm 0.07 \times 10^{-4}\,cm\,s^{-1}$ of Ni-NW-Pt, resulted in an enhancement on CEs after wet proofing. Wet proofing on nickel foam also decreases the soluble Ni^{2+} concentration by two orders of magnitude during 10 cycles, showing that the pretreatment significantly enhances the stability of metal cathode.

1. Introduction

Microbial fuel cell (MFC) is an emerging and promising technology for direct bioelectricity generation with simultaneous wastewater treatment [1–3]. A main challenge to scale up MFCs is the development of inexpensive cathode materials with high performance [4,5]. Thus, improving performance and reducing cost for practical application of MFCs are two main challenges that researchers should face [6].

Single-chambered membrane-less air-cathode MFCs were considered to be more practical for application than two-chamber MFCs because the membrane-less design and the direct use of oxygen from air as the electron acceptor significantly improved the overall power output and decreased the operational cost of MFCs [7,8]. In this system, the cost, performance and long-term stability of the electrodes are much more essential than other factors when it is considered for application [9,10]. Recently, we have shown a promising and very inexpensive carbon mesh for overcoming the high costs of the anode ($10–40 m^{-2}) [11]. Rozendal et al. [4] reported that the costs of anodic and cathodic matrix accounted for 9.4% and 47% of total costs, respectively, indicating that the expensive cathodic matrix restricted the scale of MFCs. Therefore, the low-cost and stable cathodic materials are needed to be investigated.

Recent researches proved that the traditional high-cost cathodic materials (such as carbon cloth) can be replaced by inexpensive metal meshes such as stainless steel mesh [12,13]. Metal meshes have many potential advantages over carbon cloth as cathodic materials including the excellent conductivity, low ohmic resistance, high mechanical strength, large volume fraction of gas-filled pores and low cost for large-scale application. Nickel-based materials have been demonstrated to give a remarkable performance as cathodes in MFCs [14] and microbial electrolysis cells [15,16]. Our previous studies reported a maximum power density of $4\,W\,m^{-3}$ when nickel foam was used solely as biocathode material in a two chambered MFC. However, the Ni^{2+} concentration of catholyte increased from 0.1 to $0.5\,mg\,L^{-1}$ at the end of a fed batch cycle, showing that the slow corrosion was taken place at the cathode [17]. In addition, the similar corrosion phenomenon was also reported in the microbial electrolysis cells [15,18]. Although the nickel has been used as the cathodic material of MFCs, the corrosion resistance and long-term stability of nickel electrode had not been examined in these studies.

It had been reported that the performance of air cathode can be improved by applying different coatings (such as carbon cloth and stainless steel mesh) because of the preventing the water leakage of air cathode matrix and the decreasing the water flooding of the catalyst [12,19]. The inexpensive polytetrafluoroethylene (PTFE) was the most widely used with the advantages of strong,

* Corresponding author. Tel.: +86 451 86283068; fax: +86 451 87162150.
E-mail address: yujief@hit.edu.cn (Y. Feng).

0378-7753/$ – see front matter © 2011 Elsevier B.V. All rights reserved.
doi:10.1016/j.jpowsour.2011.09.078

resistant to acids, bases, solvents, hydrophobic and oxygen permeable, making it possible to be applied as the wet proofed coating to improve the stability of the mesh surface. In this study, PTFE was used to make a wet proofed coating on the surface of nickel foam. By comparing non-wet proofed and wet proofed nickel foam as a substitute for the commonly used expensive carbon cloth as the electrode matrix in single-chambered air-cathode MFCs, the performance of MFCs using Pt catalyst were individually investigated. The performance and the stability were evaluated in terms of power production, Coulombic efficiencies (CEs), corrosion inhibition efficiency, corrosion potential and Ni^{2+} concentration during the tested period.

2. Materials and methods

2.1. Cathodes

The air-cathodes used here were composed of the electrode matrix (nickel foam, wet proofed or non-wet proofed), the catalyst (Pt) and the diffusion layers (four-coating PTFE). The nickel foam of 110 openings per square inch (110 PPI, surface density: 380 g m^{-2}, thickness: 1.6 mm, Canafull Industry Co., LTD) was either used as supplied by the manufacturer (non-wet proofed) or coated with PTFE (wet proofed). The wet proofing was performed by applying 30 wt% PTFE solution (32 μL cm^{-2} of the electrode matrix) onto the nickel foam, air-drying at room temperature for 2 h, followed by a heating at 370 °C for 0.5 h. On the air facing side of each cathode, one carbon base layer and four PTFE diffusion layers were applied as previously described [19]. Pt/C (0.35 mg cm^{-2}, C1-10 10% HP Pt on Vulcan XC-72, BASF, USA) was then applied onto the nickel foam (wet proofed or non-wet proofed) with Nafion binder according to the procedure reported by Cheng et al. Carbon cloth (CC, B-1 Designation B, 30% PTFE-based wet proofed, Clean Fuel Cell Energy, LLC, USA) cathodes with Pt catalyst (0.35 mg Pt cm^{-2}, Nafion binder) were made as the controls [19].

2.2. MFC configuration and operation

According to the previous studies, single-chambered air-cathode cubic-shaped MFCs with an electrode spacing of 4 cm were constructed and operated at 1000 Ω external resistor except as noted [8] in a 30 °C constant temperature room. The anodes were made of non-wet proofed carbon cloth (E-TEK, USA). Reactors were inoculated with the effluent (acclimated from the primary clarifier overflow of the local wastewater treatment plant) of an MFC operated for over 1 year using acetate (1.0 g L^{-1}) as fuel and fed with artificial wastewater containing acetate (1.0 g L^{-1}) as an energy and carbon source. 50 mM phosphate buffer solution (PBS, pH 7.0) containing (per liter deionized water): KCl, 0.13 g L^{-1}; $NaH_2PO_4{\cdot}2H_2O$, 3.32 g L^{-1}; $Na_2HPO_4{\cdot}12H_2O$, 10.32 g L^{-1}; NH_4Cl, 0.31 g L^{-1}, and metal (12.5 mL) and vitamin (5 mL) solutions [20] was added to increase the conductivity and buffering capacity. All the reactors were refilled with fresh media each time when the voltage decreased to less than 30 mV forming one complete cycle of operation. Each reactor had a duplicate.

2.3. Chemical and electrochemical analysis

Energy dispersive X-ray spectroscopy (EDS) was performed to analyze the elemental composition (15 kV) using a Hitachi-S-4700 analyzer coupled to a scanning electron microscope (SEM, Hitachi Ltd. S-4700) [21]. The corrosion resistances were measured using the potentiodynamic polarization technique in a single-chambered electrochemical cell (4 cm in length, 3 cm in diameter). The cell was consisted of a working electrode (tested nickel electrode, 7 cm^2 of projected surface area), a counter electrode (Pt plate), and an Ag/AgCl reference electrode (Spsic-Rex Instrument Factory, China), with the working electrode exposed to a 50 mM PBS solution (pH 7.0). The polarization curves of corrosion were obtained starting from open circuit potential (OCP) up to 0.2 V (anodic Tafel plot) versus open circuit potential (OCP) and down to −0.4 V (cathodic Tafel plot, vs. OCP) at the scan rate of 1 mV s^{-1} using a potentiostat (model 263A, AMETEK-AMT, USA) [22]. Linear polarization resistance was also measured using the potentiostat, with the scanning potentials varied from −0.020 V to +0.020 V versus OCP of working electrode at a scan rate of 0.5 mV s^{-1} [23]. The measurement of oxygen permeability was conducted by fixing a non-consumptive fiber optic dissolved oxygen (DO) probe (FOXY, Ocean Optics Inc., Dunedin, FL) into the center of the 4 cm cubical reactor filling with deionized water. The water used for DO tests was degassed by stirring in a glovebox (mini MACS, DWS) for at least 48 h to remove oxygen. Before each measurement, the probe was calibrated by two point method [24]. Ni^{2+} concentration was analyzed via inductively coupled plasma atomic emission spectroscopy (ICP-AES; Optima 5300DV, Perkin-Elmer, MA).

2.4. Calculations

The corrosion potential (E_{corr}, V) was obtained from the Tafel plots. The slope of the linear polarization resistance at corrosion potential was obtained as polarization resistance R_p (Ω cm^2). Cell voltages (E, V) across external resistors were collected and recorded with a time interval of 30 min using a data acquisition system (PISO-813, ICP DAS Co., Ltd.) connected to a personal computer. Current density ($i = E/AR$) (i, A m^{-2}) and power density ($P = iE$) (P, W m^{-2}) were calculated as previously described, where R (Ω) is the external resistor, A (m^2) is the projected surface area of the cathode [19]. Coulombic efficiency (CE) was calculated according to $CE = Q_r/Q_{th} \times 100\%$, where Q_r (C) is calculated by integrating current over time in a complete cycle and Q_{th} (C) is the theoretical amount of Coulombs calculated based on the COD removal. To obtain the polarization curves and power density curves as a function of current, different external resistors were applied in a complete batch cycle, with a series of resistances varied from the open circuit voltage (OCV) to 50 Ω in decreasing order every 30 min. Oxygen permeability of the cathode was measured in term of the mass transfer coefficient, k_0 (cm s^{-1}), by measuring the DO concentrations over time using the mass balance [19]:

$$k_0 = -\frac{v}{At}\ln\left[\frac{C_o - C}{C_o}\right] \quad (1)$$

where v (mL) is the liquid volume of the reactor (28 mL), C_o (mg L^{-1}) is the saturated oxygen concentration at 30 °C (7.6 mg L^{-1}), and C (mg L^{-1}) is the DO concentration of the solution at time t (s). The inhibition efficiencies (IE%) were calculated from polarization curves of corrosion according to

$$IE\% = \frac{100 \times (i^o_{corr} - i_{corr})}{i^o_{corr}} \quad (2)$$

where i^o_{corr} (A cm^{-2}) is the corrosion current in the absence of the corrosion inhibitor (PTFE), i_{corr} (A cm^{-2}) is the corrosion current in the presence of the inhibitor [22].

3. Results and discussion

3.1. Characteristics of different nickel foam cathodes

SEM images showed that porous cell structures of the wet proofed nickel foam were well covered by PTFE (Fig. 1C and D), while the non-wet proofed nickel foam had a porous three-dimensional network as the physical property of the material itself (Fig. 1A and B). The EDS results (Table S1) showed that the surface of

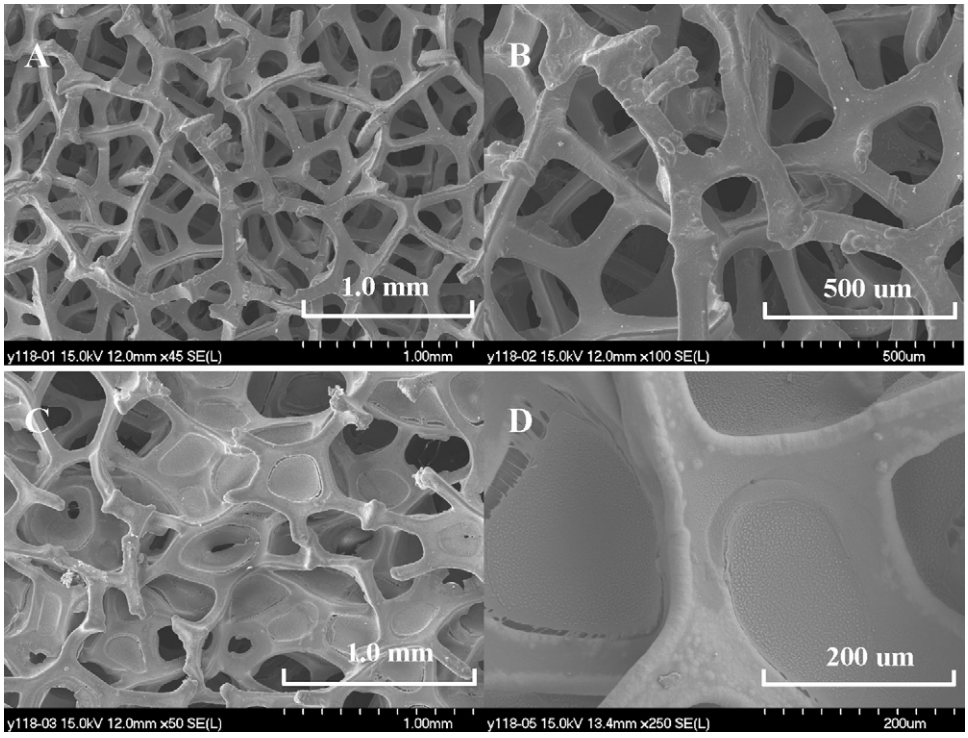

Fig. 1. Scanning electron microscope (SEM) images of non-wet proofed matrix (A, 45×; B, 100×) and wet proofed matrix (C, 50×; D, 250×) of nickel foam.

the wet proofed nickel foam was composed of C (49.65%), F (30.65%) and Ni (19.69%) compared with 100% Ni of the non-wet proofed nickel foam, which was in agreement with SEM images in Fig. 1.

3.2. Corrosion inhibition efficiency

The corrosion inhibition efficiency of nickel foam was evaluated when PTFE was used as the inhibitor facing to the corrosion medium (50 mM PBS). Potentiodynamic polarization behavior (Fig. 2A) showed a significant change on E_{corr} value of nickel foam in the absence and presence of wet proofing. Wet proofing on nickel foam drove the corrosion potential by more than 0.15 V towards the positive direction, showing that the corrosion was effectively inhibited after wet proofing, which was in accordance with previously studies [25,26]. The corrosion current of the wet proofed nickel foam was significantly decreased from 0.66 μA to 0.018 μA compared with non-wet proofed nickel foam, indicated that the wet proofed nickel foam in 50 mM PBS impeded the development of aggressive conditions and reduced the dissolution of metal. The polarization resistance (R_p) values were determined from the slopes of the potential versus current plots (Fig. 2B). With Pt catalyst, the wet proofing increased the R_p of nickel foam by 273% from 41 to 153 Ω cm^2 with an IE of 97% (PTFE as inhibitor), indicated that the PTFE coating effectively inhibited the corrosion.

3.3. Performance of MFCs using different cathodes

The period of inoculation lasted for 100–150 h. MFCs with different cathodes produced repeatable voltages. Using Pt as the cathode catalyst, similar voltages of 510 ± 4 mV were obtained in MFCs using both Ni-W-Pt and carbon cloth with Pt catalyst (CC-Pt) cathodes, which were 11% higher than that of Ni-NW-Pt (460 ± 5 mV). Not as the repeatable voltages obtained in MFCs using Ni-W-Pt and CC-Pt, the maximum voltages of Ni-NW-Pt were slowly decayed after several feeding cycles. This could be attributed to the negative effect of the Ni^{2+} generated from the corrosion of cathode matrix (see below) on the metabolic activity of anodic bacteria during start-up period (Fig. S1).

According to the polarization curves (Fig. 3A), the same maximum power density of 0.68 ± 0.02 W m^{-2} was observed in MFCs using Ni-W-Pt and CC-Pt, which was 35% larger than the power density obtained with Ni-NW-Pt (0.51 ± 0.02 W m^{-2}). Potential analysis (Fig. 3B) showed that the increase on maximum power densities were attributed to the more negative anode potentials and more positive cathode potentials observed in Ni-W-Pt than those obtained in Ni-NW-Pt over the current density range from 0 to 3.7 A m^{-2}. The reason for the decrease on anode performance of Ni-NW-Pt could be the biological toxicity of relative high concentration of Ni^{2+} (see below). Although the oxygen mass transfer coefficient of Ni-W-Pt was lower than that of Ni-NW-Pt due to wet proofing, the cathode potential of the Ni-W-Pt was higher than that of Ni-NW-Pt. This could be attributed to the loss of surface conductivity when the serious corrosion had taken place on the cathode of Ni-NW-Pt.

Applying PTFE coating on the nickel foam cathode slightly increased CEs (Fig. 4). The CEs of Ni-NW-Pt were varied from 24% to 51% depending on the external resistance. Within the same range of resistance, comparable CEs varied from 29% to 63% were observed in MFCs using Ni-W-Pt and CC-Pt. The maximum CE of 62% was obtained at an external resistance of 100 Ω in the MFC with Ni-W-Pt, which is over 22% higher than that of MFCs using Ni-NW-Pt (51%) at the same resistance. Higher CEs achieved by MFCs using wet proofed nickel foams indicated that the wet proofing effectively reduced the oxygen diffusion through the cathode [8,27].

3.4. Oxygen permeability of the cathodes

The oxygen mass transfer coefficient (k) of Ni-W-Pt was 0.68 ± 0.06 × 10^{-4} cm s^{-1}, which was 53% lower than 1.46 ± 0.07 × 10^{-4} cm s^{-1} of Ni-NW-Pt, showing that the application of the wet proofing decreased oxygen permeation. The control cathode of CC-Pt with four PTFE diffusion layers had an oxygen

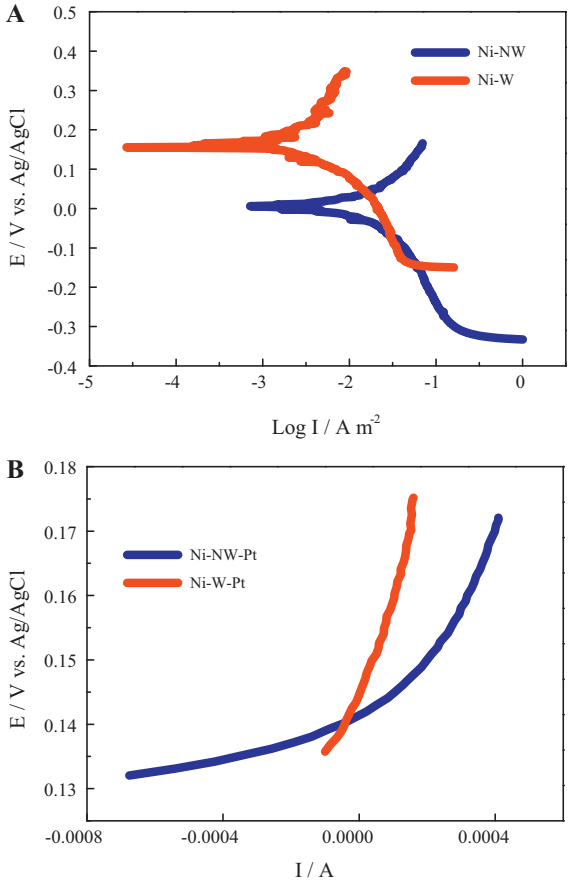

Fig. 2. (A) Potentiodynamic polarization behavior of nickel foam in 50 mM PBS. Ni-NW: the non-wet proofed nickel foam, Ni-W: the wet proofed nickel foam. (B) Linear polarization plots in the presence and absence wet proofed PTFE coating of nickel foam in 50 mM PBS. Ni-W-Pt: the wet proofed nickel foam with Pt catalyst; Ni-NW-Pt: the non-wet proofed nickel foam with Pt catalyst.

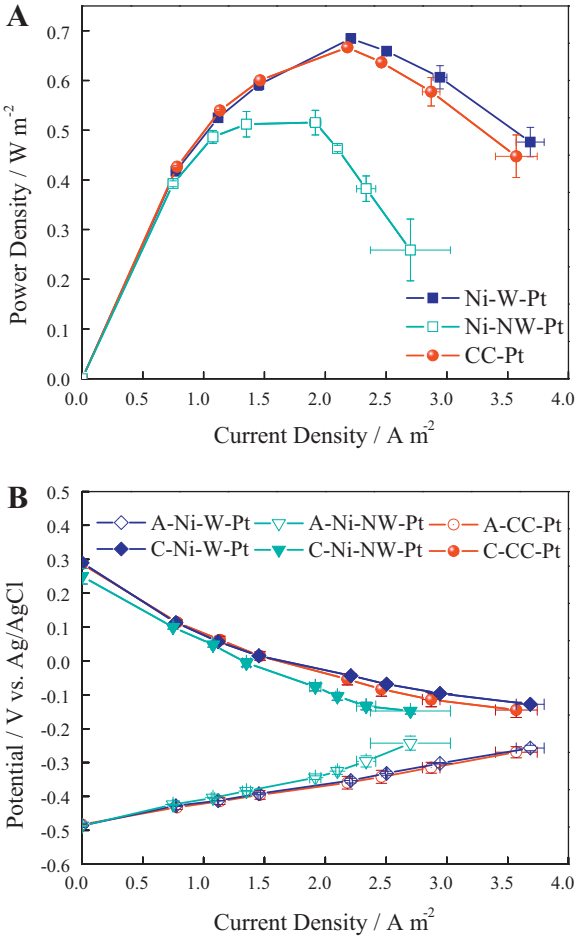

Fig. 3. Power densities (A) and electrode potentials (B) of MFCs using different cathodes (Ag/AgCl, 195 mV vs. SHE). CC-Pt: the carbon cloth cathode with Pt catalyst; Ni-W-Pt: the wet proofed nickel foam cathode with Pt catalyst; Ni-NW-Pt: the non-wet proofed nickel foam cathode with Pt catalyst. Error bars ± SD were based on averages measured in triplicate.

transfer coefficient of $1.11 \pm 0.08 \times 10^{-3}$ cm s^{-1}, with a value comparable to $1.2 \pm 0.1 \times 10^{-3}$ cm s^{-1} as previously reported [12]. The k value of CC-Pt was significantly higher than that obtained using the nickel foam cathode, which could be due to the difference in matrix thickness (carbon cloth 0.7 mm; nickel foam 1.6 mm).

3.5. Stability of the cathodes

All the cathodes were examined for possible corrosion by measuring Ni^{2+} concentrations in continuous 10 cycles during the period of start-up (Fig. 5A). The soluble Ni^{2+} concentration of the Ni-W-Pt rapidly decreased from 0.98 to 0.15 mg L^{-1} over the initial 3 cycles and then further decreased from 0.15 to 0.01 mg L^{-1} in the following 3 cycles. Higher Ni^{2+} concentrations of 1.60–0.40 mg L^{-1} were observed in MFCs using Ni-NW-Pt in first 6 cycles, which was consistent with 0.5 mg L^{-1} obtained in a non-wet proofed nickel foam biocathode [17]. The Ni^{2+} concentration of Ni-W-Pt stabilized at a relative constant value of 0.01 mg L^{-1} at cycle 10, while the Ni^{2+} concentration in MFCs using Ni-NW-Pt was gradually decreased to *ca.* 0.16 mg L^{-1} at cycle 10. Wet proofing by PTFE on nickel foam decreased the Ni^{2+} concentration in solution during 10 cycles (from cycle 1 to cycle 10) by two orders of magnitude, showing that the pretreatment significantly enhanced the stability of nickel foam cathode.

The long-term stability of the cathodes was also investigated after the MFCs were stably operated for 60 days. The Ni^{2+} concentration of the Ni-NW-Pt was higher than the Ni-W-Pt over an external resistance range from 1000 to 100 Ω (Fig. 5B), corresponded with a more negative cathode potential observed in Fig. 3B. It can be thermodynamically calculated from $\Delta G = -n\,\Delta E\,F$, more negative electrode potential makes the corrosion more thermodynamically favorable, where ΔE is the potential difference in redox

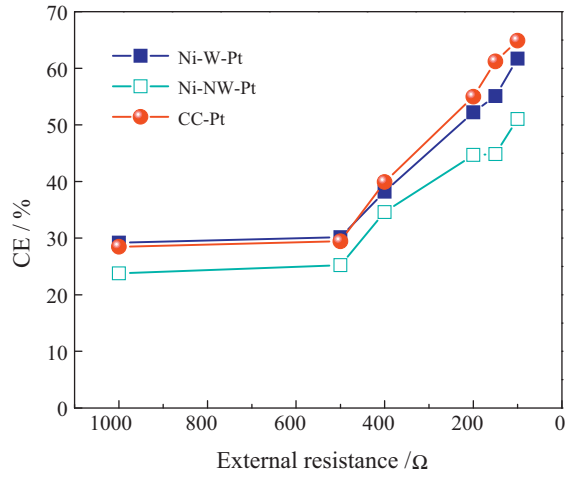

Fig. 4. Coulombic efficiencies (CEs) as a function of external resistances for MFCs using different cathodes.

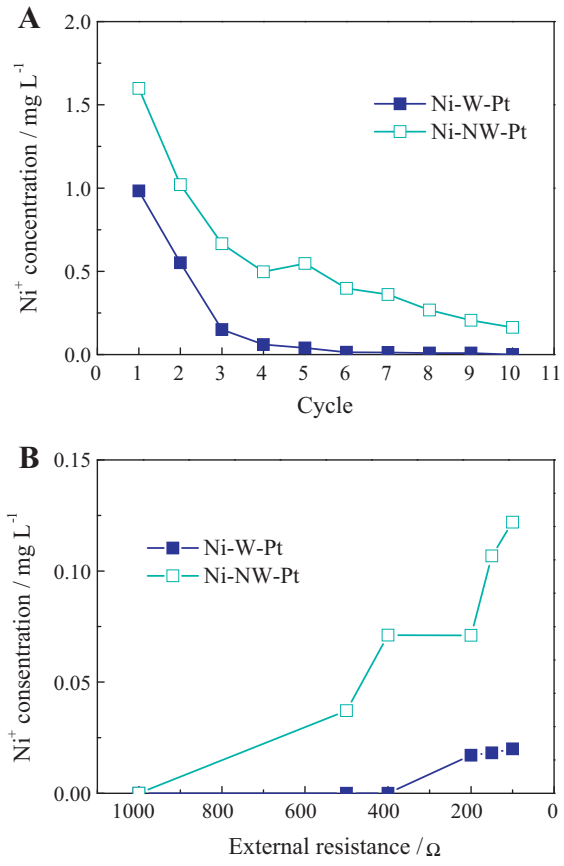

Fig. 5. Ni^{2+} concentration in solution of MFCs with different cathodes in initial 10 cycles (A) and Ni^{2+} concentrations as a function of external resistance for MFCs using different cathodes (B).

potential of Ni/Ni^{2+} and electron acceptor (cathode potential), F is the Faraday constant, n is the mole of electron transferred (2 for Ni corrosion). Thus, the primary mechanism of Ni^{2+} corrosion could be due to the relative negative cathode potentials. In addition, the O_2 reduction on Pt/C catalyst possibly occurred at more negative potentials ($E < 0.3\ V_{RHE}$) on trace of hydrogen peroxide formation [28,29], which made the corrosion of Ni more serious.

4. Conclusions

The application of wet proofed PTFE coating on nickel foam exhibited a corrosion inhibition efficiency of 97%. The use of wet proofed nickel foam as cathodic matrix (Pt catalyst) in an MFC produced a maximum power density of $0.69 \pm 0.01\ W\ m^{-2}$, which was 35% higher than that obtained in MFCs with non-wet proofed cathode (Ni-NW-Pt). The oxygen mass transfer coefficients of the wet proofed cathodes were lower than those of non-wet proofed cathode, resulted in the enhancement of CEs. Ni^{2+} concentrations measured in solution demonstrated that wet proofing on the matrix increased the erosion resistance of nickel foam when it was utilized as cathodic matrix. The results indicated that the wet proofing was a promising method to enhance the stability and performance of metal cathodic matrix in MFCs.

Acknowledgements

The research was supported by the State Key Laboratory of Urban Water Resource and Environment, Harbin Institute of Technology (2009TS03). The authors also thank the National Innovation Team supported by the National Science Foundation of China (No. 50821002).

Appendix A. Supplementary data

Supplementary data associated with this article can be found, in the online version, at doi:10.1016/j.jpowsour.2011.09.078.

References

[1] B.E. Logan, Nat. Rev. Microbiol. 7 (2009) 375–381.
[2] K. Rabaey, W. Verstraete, Trends Biotechnol. 23 (2005) 291–298.
[3] D.R. Lovley, Curr. Opin. Biotechnol. 19 (2008) 564–571.
[4] R.A. Rozendal, H.V.M. Hamelers, K. Rabaey, J. Keller, C.J.N. Buisman, Trends Biotechnol. 26 (2008) 450–459.
[5] Y. Zuo, S. Cheng, B.E. Logan, Environ. Sci. Technol. 42 (2008) 6967–6972.
[6] B.E. Logan, Appl. Microbiol. Biotechnol. 85 (2010) 1665–1671.
[7] X.Y. Zhang, S.A. Cheng, P. Liang, X. Huang, B.E. Logan, Bioresour. Technol. 102 (2011) 372–375.
[8] H. Liu, B.E. Logan, Environ. Sci. Technol. 38 (2004) 4040–4046.
[9] M. Zhou, M. Chi, J. Luo, H. He, T. Jin, J. Power Sources 196 (2011) 4427–4435.
[10] S. Cheng, H. Liu, B.E. Logan, Environ. Sci. Technol. 40 (2006) 364–369.
[11] X. Wang, S.A. Cheng, Y.J. Feng, M.D. Merrill, T. Saito, B.E. Logan, Environ. Sci. Technol. 43 (2009) 6870–6874.
[12] F. Zhang, T. Saito, S.A. Cheng, M.A. Hickner, B.E. Logan, Environ. Sci. Technol. 44 (2010) 1490–1495.
[13] F. Zhang, M.D. Merrill, J.C. Tokash, T. Saito, S. Cheng, M.A. Hickner, B.E. Logan, J. Power Sources 196 (2011) 1097–1102.
[14] F. Zhang, S.A. Cheng, D. Pant, G. Van Bogaert, B.E. Logan, Electrochem. Commun. 11 (2009) 2177–2179.
[15] A.W. Jeremiasse, H.V.M. Hamelers, M. Saakes, C.J.N. Buisman, Int. J. Hydrogen Energy 35 (2010) 12716–12723.
[16] P.A. Selembo, M.D. Merrill, B.E. Logan, J. Power Sources 190 (2009) 271–278.
[17] X. Wang, Y. Feng, E. Wang, C. Li, J. Biotechnol. 136S (2008) S662.
[18] P.A. Selembo, M.D. Merrill, B.E. Logan, Int. J. Hydrogen Energy 35 (2010) 428–437.
[19] S. Cheng, H. Liu, B.E. Logan, Electrochem. Commun. 8 (2006) 489–494.
[20] D.R. Lovley, E.J.P. Phillips, Appl. Environ. Microbiol. 54 (1988) 1472–1480.
[21] J. Liu, Y. Feng, X. Wang, X. Shi, Q. Yang, H. Lee, Z. Zhang, N. Ren, J. Power Sources (2011) 8409–8412.
[22] K.F. Khaled, Mater. Chem. Phys. 112 (2008) 104–111.
[23] C. Jeyaprabha, S. Sathiyanarayanan, S. Muralidharan, G. Venkatachari, J. Braz. Chem. Soc. 17 (2006) 61–67.
[24] X. Wang, Y.J. Feng, J. Liu, H. Lee, C. Li, N. Li, N.Q. Ren, Biosens. Bioelectron. 25 (2010) 2639–2643.
[25] H. Bhandari, V. Choudhary, S.K. Dhawan, Synth. Met. 161 (2011) 753–762.
[26] A. Oncul, K. Coban, E. Sezer, B.F. Senkal, Prog. Org. Coat. 71 (2011) 167–172.
[27] Y.Z. Fan, H.Q. Hu, H. Liu, J. Power Sources 171 (2007) 348–354.
[28] A. Schneider, L. Colmenares, Y.E. Seidel, Z. Jusys, B. Wickman, B. Kasemo, R.J. Behm, Phys. Chem. Chem. Phys. 10 (2008) 1931–1943.
[29] M. Inaba, H. Yamada, J. Tokunaga, A. Tasaka, Electrochem. Solid State Lett. 7 (2004) A474–A476.